

Atomic densities of states near Si (111) surfaces

K. C. Pandey and J. C. Phillips

Bell Laboratories, Murray Hill, New Jersey 07974

(Received 5 August 1974)

The semiempirical tight-binding method is used to construct accurate valence bands for bulk Si and Ge using Hamiltonian parameters through second neighbors. One additional parameter is used to describe surface relaxation (back-bond contraction). The density of surface bands and resonances associated with atomic layers near the surface is calculated. Surprisingly, the resonances are found to contribute to the surface density of states almost as effectively as proper surface states. Comparison with ion-neutralization, electron-energy loss, and ultraviolet photoemission data is made.

The electronic properties of Si and Ge semiconductor surfaces are dominated by two kinds of surface states: dangling-bond states, which lie in the energy gap between valence and conduction bands, and back-bonding states, which lie within and below the bulk valence band. In two earlier publications^{1,2} we have developed a semiempirical tight-binding method (SETBM) for calculating these states, and have claimed that the results of the SETBM were comparable to those obtained in a "first-principles" self-consistent calculation by Appelbaum and Hamann³ (AH). The SETBM requires, in addition to the parameters used to fit the bulk valence bands, one parameter to describe the band broadening effects of bond shortening that take place when the surface relaxes. In this paper we report atomic densities of states for unreconstructed relaxed and unrelaxed Si (111) surfaces. With these densities of states the "self-consistent" character of the SETBM can be compared with that of the AH pseudopotential calculation and with experiment. The results of this comparison suggest that while the AH calculation gives results in very good agreement with experiment, our results are even better. Because the SETBM is also much more economical than the numerical methods employed by AH, we expect the SETBM to be extremely useful in describing the properties of real (reconstructed) semiconductor surfaces. The SETBM also makes direct connection with molecular-orbital methods, especially complete neglect of differential overlap,⁴ and so should be extremely useful in treating chemisorbed impurities.

The bulk energy bands are fitted by tight-binding parameters based on orthogonalized atomic orbitals $\Psi_j(\vec{r} - \vec{R}_m)$, where j is an s or p atomic orbital and \vec{R}_m is an atomic site. Each wave function in the films (here 20 atomic layers in thickness) studied is represented by

$$\varphi_{\mathbf{k}_s, n} = \sum_{j, m} e^{i\mathbf{k}_s \cdot \vec{R}_m} a_{\mathbf{k}_s, n}^{j, m} \Psi_j(\vec{r} - \vec{R}_m) \quad (1)$$

where \mathbf{k}_s is the surface wave vector, and n is a

surface band index. The density of states $\rho_m(E)$ on the atom at the m th atomic site is given by

$$\rho_m(E) = \sum_{j, \mathbf{k}_s, n} |a_{\mathbf{k}_s, n}^{j, m}|^2 \delta(E_{\mathbf{k}_s}^j - E). \quad (2)$$

The values of $\rho_m(E)$ were obtained by sampling a grid of 53 points \mathbf{k}_s in the Brillouin zone to determine φ and E . The basic sample of 53 points (not equivalent by symmetry) was augmented by a factor of 200 by linear interpolation, and the total sample was used to construct histograms for $\rho_m(E)$. The latter was then smoothed with a half width of 0.05 eV. The bulk tight-binding parameters used here and in earlier work² for Si and Ge are listed in Table I. The details of the fitting procedure and comparison with other calculations as well as experiment are given in Appendix A.

We can calculate the Fermi energy from $\rho_m(E)$ by summing over all m in the film and integrating over E from below the valence band up to E_F , which is fixed by having on the average, four valence electrons per Si atom in the film. The values of E_F (relative to the valence band maximum) are 0.46 and 0.00 eV, for relaxed and unrelaxed surfaces, respectively. In Table II, the number N_m of valence electrons per Si atom in the m th layer is given for the two surfaces. This number oscil-

TABLE I. Tight-binding parameters for bulk Si and Ge (in eV). The subscripts 1 and 2 refer to first and second neighbors. Note the systematic progression of the first-neighbor parameters.

	Si	Ge
E_s	0.00	0.00
E_p	4.39	6.44
$(ss)_1$	-2.08	-1.69
$(sp\sigma)_1$	-2.12	-2.03
$(pp\sigma)_1$	-2.32	-2.55
$(pp\pi)_1$	-0.52	-0.67
$(pp\sigma)_2$	-0.58	-0.41
$(pp\pi)_2$	-0.10	-0.08

lates near four and, for a pair of atoms which are nearest neighbors, averages almost exactly to four. Each pair of (111) layers (which, if coplanar, would have the graphite structure) is almost neutral and has a small dipole moment; the contributions of these dipole moments to the difference between the inner and outer potentials are 0.14 and 0.57 eV (relaxed and unrelaxed, respectively). This can be compared with an *a priori* estimate⁵ of an upper limit of about 2 eV.

The atomic densities of states for atoms in the first and fourth layers of a relaxed Si (111) surface (0.33 Å contraction) are compared with the bulk density of states in Fig. 1. Densities of states were obtained for atoms in all layers of a 20-layer (111) film with the surface layer relaxed (as above) or unrelaxed. The density of states of the fourth layer is shown in Fig. 1 because it contains an intriguing (and unexpected) echo of the dangling bond states (about $\frac{1}{5}$ as large as the first layer) which are negligible in other layers.

A number of interesting features of $\rho_m(E)$ for $m=1$ (first layer) are indicated in Fig. 1. One can define a two-dimensional density of states for each back-bond surface band,² and associated with (maxima or minima) or saddle points in the surface bands one finds step function or logarithmic singularities in the two-dimensional densities of states. Echoes of these two-dimensional singularities are found in the atomic densities of states, especially for atoms in the first layer ($m=1$). These echoes are indicated in Fig. 1. We have previously indicated² that the features in electron-energy-loss spectra (ELS) denoted by S_2 and S_3 by Rowe and Ibach⁶ are associated with the surface band 2 and surface band 4 minima, as indi-

cated in Fig. 1. The minimum for band 3 falls close to the saddle-point peak labeled 3 in Fig. 1, as one can see from our earlier description² of the surface bands. The S_2 and S_3 structure is associated with excitation of electrons primarily in the first and second layers to final states in the conduction band near +2.0 eV (bulk valence-band maximum=0.0 eV). Excitation of electrons from peak 3 in Fig. 1 to final states near +2.0 eV would produce structure in ELS near 10.5 eV, which is difficult to distinguish from losses caused by creation of surface plasmons.

The atomic densities of states shown in Fig. 1 refer to the relaxed but unreconstructed (111) surface. Well defined structure in ELS has been observed for (111) 2×1 and (111) 7×7 surfaces (cleaved and annealed surfaces, respectively). For this reason it is perhaps not surprising that the saddle-point peaks labeled 2 and 4 in Fig. 1 also have not shown up in ELS. The structure associated with these saddle-point peaks may be broadened more than that associated with step functions (derived from surface band minima) when account is taken of the effects of reconstruction and strain fields associated with surface steps, etc.

One can define a mean electron ion energy per atom located at $\vec{R} = \vec{R}_m$ by

$$E_m = \int_{E_0}^{E_F} \rho_m(E)(E - E_0) dE \quad (3)$$

We have measured E from the bottom of the bulk valence band ($E_0 = -12.5$ eV relative to the top of the valence band). Because four electrons per atom contribute to E_m , the value of E_m is about $4 \times \frac{3}{5} |E_0|$, or about 30 eV. The dependence of E_m

TABLE II. Variation of electron density from layer to layer in the relaxed and unrelaxed configurations. Note that the effect of relaxation is to reduce the large excess of electrons in the first layer and replace them with a dipolar distribution in the first and second layers, which is reflected in a weaker dipole in the third and fourth layers.

Layer	Relaxed			Unrelaxed		
	N_m (electrons/atom)	E_m (eV/atom)	E_m/N_m	N_m (electrons/atom)	E_m (eV/atom)	E_m/N_m
Bulk	4.00	29.29	7.32	4.00	29.29	7.32
1	4.19	31.14	7.43	4.43	37.69	8.51
2	3.84	24.31	6.33	3.98	29.10	7.31
3	3.95	28.34	7.17	3.93	28.33	7.21
4	4.04	30.00	7.43	3.99	29.22	7.32
5	3.99	29.15	7.31	3.98	29.03	7.29
6	3.99	29.20	7.32	3.99	29.13	7.30
7	4.00	29.28	7.32	3.99	29.19	7.32
8	4.00	29.28	7.32	3.99	29.23	7.33
9	4.00	29.29	7.32	4.00	29.24	7.31
10	4.00	29.29	7.32	4.00	29.25	7.31
Total (10 Layers)	40.00	289.28		40.25	299.41	

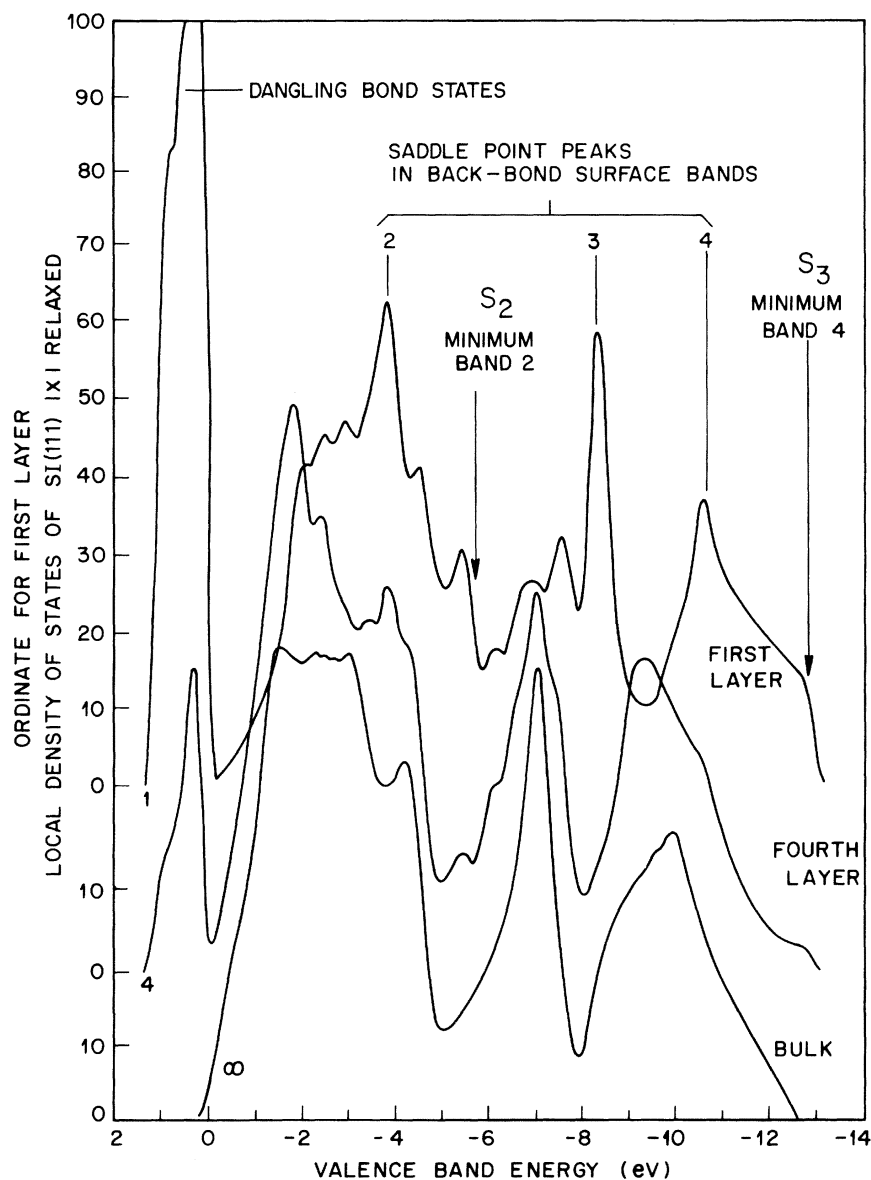


FIG. 1. Atomic densities of states of a relaxed, unreconstructed Si(111) surface are compared with the bulk density of states. For the most part the atomic densities of states of layers other than the fourth tend monotonically from that of the first layer to the bulk at a rate similar to that shown for the average energy in Table II. The fourth layer is an exception insofar as it exhibits a larger density of dangling bond states ($E > 0$) than the second and third layers. This is because the atoms in the fourth layer exhibit a bond configuration which exactly mirrors that of the first layer without translation of atomic coordinates parallel to the surface.

on m is another measure of the extent to which $\rho_m(E)$ differs from the bulk density of states $\rho_0(E)$. Note that electron-electron energies are counted twice in determining E , and it does not include ion-ion energies. Thus although we have listed the total energy $E = \sum E_m$ ($m=1-10$) in Table II, it cannot be simply compared to ten times the bulk E/atom to estimate, e.g. surface energies (which are of the order⁷ of 0.5 eV/surface atom). We have also listed in Table II the quantity E_m/N_m , which converges somewhat more rapidly than E_m to the bulk value.

The value for E_F used for the unrelaxed lattice (0.0 eV, i.e., the top of the valence band) gives 0.25 (out of 40) excess electrons, because the dangling bond surface bands overlap the bulk va-

lence bands. This condition could be corrected by shifting the diagonal energy of the surface atom upwards by about 0.1 eV (a kind of band bending on an atomic scale). Alternatively, one can remove 0.25 electrons from the dangling bond surface states, at an energy 12.5 eV above the bottom of the valence band, corresponding to a reduction in the total energy $\sum E_m$ of 3.1 eV. Because the unrelaxed configuration is unrealistic, we have not pursued this question further.

It is customary in discussing photoemission data to interpret energy distributions of emitted electrons produced by photons of energy 20–30 eV in terms of an "optical density of states" (ODS) of the valence band of the bulk crystal.⁸ In this picture several simplifying assumptions are made:

first, that oscillator strengths to final states at these photon energies vary slowly with initial energy $E_i(\mathbf{k})$, when averaged over different Bloch momenta \mathbf{k} , and second, that except near the top of the valence band surface effects are of little importance. The validity of the first assumption has been examined⁸ by comparing theoretical bulk densities of states with calculated energy distributions (including the effects of oscillator strengths, transport, and escape); overall good agreement is found, although in the π electron region (-4 – 0 eV, where 0 eV is the valence-band maximum) there are variations in peak heights.

Surface effects are the second question. Most studies⁸ employ unannealed natural cleavage faces, which if metastable probably exhibit large reconstruction effects⁹; similarly less stable faces may also exhibit large surface effects, such as those already observed by Rowe and Ibach¹⁰; the surface effects are particularly pronounced in the π electron region. In order to interpret these surface effects, and to separate them properly from bulk effects, it is necessary to study the variation of the electronic density of states near the surface of the crystal. The estimated escape depths of excited valence electrons for photons in the energy range 15 – 30 eV are 7 – 15 Å (5 – 10 atom layers),^{11–13} and we find significant variations of the density of states in this region.

To illustrate the effect of an average escape depth l on the ODS, we have calculated the occupied density of states

$$N(e, l) = \sum_m \rho_m(E) e^{-Z_m/l} \Theta(E - E_F) \quad (4)$$

where Z_m is the depth below the surface of the site located at $R=R_m$, with $Z_1=0$ and $\Theta(x)=1$ for $x<0$ and 0 for $x>0$. The behavior of $N(E, l)$ for two values for l , 3 and 13 Å, is shown in Fig. 2 after smoothing by 0.2 eV. Overall the differences are

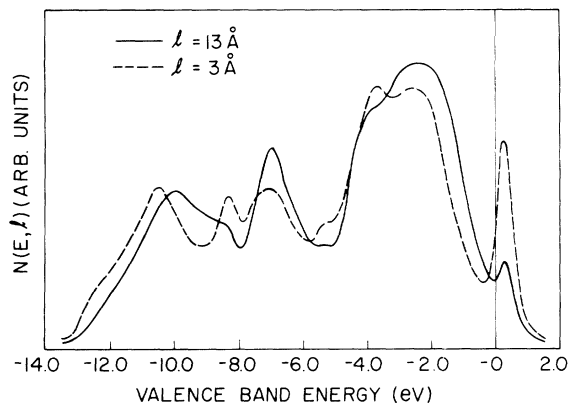


FIG. 2. Weighted averages of the atomic densities of states with different escape depths [see Eq. (4)].

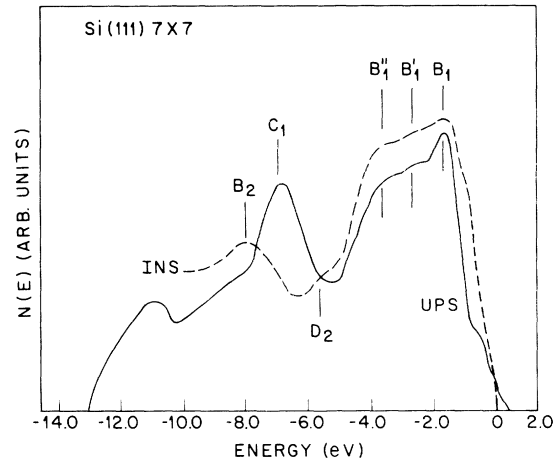


FIG. 3. Comparison of valence band density of states obtained from well cleaved, annealed, oxygen-free Si (111) reconstructed 7×7 surfaces.^{14,16} The experimental spectra in the region near -2 eV have been aligned.¹⁵ Differences in the features C_1 , D_1 , and D_2 are discussed in the text.

significant, but they are considerably less than the observed¹⁰ differences between Si (111) 2×1 and 7×7 reconstructed surfaces. This suggests that the lateral motion of atoms in the first and second layers associated with the cleaved 2×1 and annealed 7×7 patterns must be quite large.⁹ For this reason comparison of our calculated curves of $N(E, l)$ with experimental photoemission distributions, or ODS, is not yet particularly meaningful. The sensitivity of the ODS to surface conditions is discussed in Appendix B.

In analyzing results of this kind, the reader may find it tempting to compare the strength of the dangling bond shoulder near $E=0$ (the valence-band maximum) with the bulk valence band structure which lies below it in the range -4 eV $< E < 0$. [In constructing $N(E, l)$ we have used the value of the Fermi energy, $E_F=0.46$ eV mentioned above, corresponding to one electron per dangling bond.] We have not made such a comparison because we feel that the localization of electrons in the dangling bond states is sufficiently great that effects of the Franck-Condon-type may reduce the oscillator strength for excitation of dangling bond electrons in the energy range of interest.

Because ion-neutralization spectroscopy^{14,15} (INS) is more sensitive than ultraviolet-photoemission spectroscopy^{10,16} (UPS) to the density of states in the surface layer, the two kinds of spectra are compared in Fig. 3. In the π electron region (-4 eV $< E < 0$) the two curves are quite similar. At lower energies several differences are apparent. The UPS peak near -6.8 eV and labeled C_1 in Fig. 3 seems to be shifted downwards in energy

in INS to about -7.8 eV; a similar shift can be seen in the energy of peak 3 in the bulk $\rho(E)$ and in the first layer $\rho_1(E)$ in Fig. 1, or by comparing $N(E, 3 \text{ \AA})$ with $N(E, 13 \text{ \AA})$ in Fig. 2. An additional feature of INS is the shoulder near -5.5 eV and labeled D_2 in Fig. 3. There is only a valley in the bulk density of states near this energy, but in $\rho_1(E)$ there is an edge associated with the minimum of surface band 2. It is possible that this edge, which we have also associated with the ELS structure labeled S_2 , can account for D_2 as well. Similarly the sharp peak in the UPS near -1.5 eV may be associated with the peak in the density of states at the third and fourth layers due to a surface resonance.

The calculations presented here are the first (to our knowledge) which give densities of states for Si near the surface with sufficient accuracy to make comparison with experiment meaningful. A moment method has been combined with an unsatisfactory bulk band structure to yield unrelaxed local densities of states.¹⁷ The weakness of the moment method is that it does not treat with sufficient accuracy the analytic singularities¹⁸ in $\rho_m(E)$ that are associated with step functions, logarithmic singularities, etc., which are important in analyzing experimental data and which are evident in the results shown in Fig. 1.

Another comparison of interest concerns our results and the first-principles calculation of Appelbaum and Haman.³ In determining E_F we have assumed that each film of N atoms contains $4N$ valence electrons. This condition of charge neutrality is equivalent to assigning one electron to each dangling bond,¹⁹ whereas AH find 0.7 electrons/dangling bond. It is possible that this discrepancy arises from their use of a matching condition between bulk and surface between the second and third layers. In Fig. 1 we saw that there is a substantial density of dangling bond states associated with the fourth layer.

One may also note that our dangling bond band width *Ansatz*,² which used $4\beta a = 3.5$,

$$H_{kl}(R_{mn}) = H_{kl}(R_{mn}^0) \exp \beta(R_{mn}^0 - R_{mn}) \quad (5)$$

places the Fermi energy E_F (with one electron per dangling bond) at approximately the correct energy (about 0.47 eV above the top of the valence band) in the relaxed configuration. In this configuration our results are in good agreement with AH who would with one electron/dangling bond place E_F at 0.35 eV. In the unrelaxed configuration (semi-infinite lattice) our value of E_F is 0.0 eV, whereas the AH E_F (both with one electron per dangling bond) is about 0.25 eV. Part of this much larger discrepancy arises from the lack of self consistency of the preliminary AH calculations in the unrelaxed configuration; more recent AH results for

the latter configuration agree with ours to within 0.05 eV.

The crucial feature of Eq. (5) is that while the first- and second-neighbor interactions are altered near the surface, the intra-atomic energies E_s and E_p are the same for atoms at the surface as for atoms in the bulk. In a homonuclear crystal this assumption is quite plausible, for it corresponds to assuming (approximately) that no charge accumulates near the surface (flat band condition). This picture is not exactly equivalent to the one of small oscillations in ρ_m which are observed in Table II, however, because of the overlap of atomic charge densities; if ρ_m were constant at ρ_0 (the bulk value), then this would correspond to neutral pseudoatoms. A superposition of neutral pseudoatom potentials does not give a good approximation to the self consistent pseudopotential near the surface.²⁰ If we were to assign a chemical potential μ_m to each atom (analogous to an electronegativity parameter), then in the tight-binding method this would depend on some weighted average of $E_s(m)$ and $E_p(m)$. Keeping $E_s(m)$ and $E_p(m)$ constant is sufficient to make μ_m nearly constant. This latter condition is much more appropriate (in the sense of the Feynmann-Hellman theorem) for a relaxed, self-consistent configuration than it is for a nonequilibrium configuration such as the semi-infinite lattice. This may explain why our results agree much better with those of AH in the relaxed case than in the unrelaxed one. Moreover, our result is independent of numerical approximations or rounding errors (such as those associated with a choice of matching plane), so that (as was mentioned earlier) it is quite possible that our results are more accurate than those of AH. Certainly in the homonuclear case we can approach the problem of self-consistency in the presence of lateral motions associated with surface reconstruction with confidence.

In conclusion, in this paper we have presented a variety of material to indicate the directions which we believe theory should follow in attempting to construct a realistic picture of the electronic structure of the relaxed surface of a covalent crystal such as Si(111). We have shown that not only surface states, but also (and perhaps surprisingly) surface resonances make the surface density of states very different from the bulk density of states for a degree of relaxation which appears to be realistic. We have connected several experimental observations (by INS¹⁴ and ELS,⁶ as well as UPS^{10,11}) with features of the surface density of states of relaxed Si. Further comparison of theory and experiment will, however, await the inclusion not only of relaxation but also of reconstruction effects as well.

ACKNOWLEDGMENTS

We have benefited from conversations with J. E. Rowe, J. A. Appelbaum, and D. R. Hamann. We are particularly grateful to Dr. Rowe for permission to present his previously unpublished data in Figs. 5(a) and 5(b).

APPENDIX A: BULK TIGHT-BINDING PARAMETERS

The semiempirical approach to the determination of parameters in a tight-binding or linear combination of atomic orbitals representation has been widely used in solids,²¹ and earlier and more extensively in molecules as the Hückel theory.²² The theory has undergone many refinements, especially in molecular calculations, for example the extended Hückel method,²³⁻²⁶ in which allowance is made explicitly for nonorthogonality of orbitals situated on different atoms.

In all semiempirical methods it is essential to reduce the number of adjustable parameters to a minimum. If one desires to fit both valence and conduction bands of a bulk semiconductor near the energy gap, the pseudopotential method, which employs three parameters per element in the unit cell, is most economical and most accurate. The dangling and back-bond surface states that we have considered are derived primarily from bulk valence band states. Thus we are concerned with achieving a good fit to the entire bulk valence band, and a fairly good fit to the lowest conduction band. Because of the localized nature of the surface states, atomic orbitals are a natural basis set for this problem.

Our procedure for fitting the bulk energy bands was to calculate forty energy levels throughout the Brillouin zone using a pseudopotential interpolation scheme. The pseudopotential parameters were adjusted to fit the experimental valence band energies marked in Figs. 4(a) and 4(b). These energies represent averages determined in a variety of recent photoemission experiments. They differ but slightly from the values which have been obtained in many pseudopotential calculations over the last 15 years. The more accurate input values have almost no effect, e.g. on surface parameters such as the dangling bond bandwidth. However, because surface structure in the density of states is always measured relative to allowed and forbidden energy intervals of the bulk band structure, comparison with photoemission experiments is greatly facilitated by an accurate fit to the bulk valence band. Our fit is somewhat more accurate than AH's fit,³ and this is one of the reasons that our calculated spectra have been found to yield consistently better agreement with experiment (by 0.1–0.3 eV). Our fit is accurate to 0.2 eV (0.3 eV) for Ge (Si) valence bands (rms error).

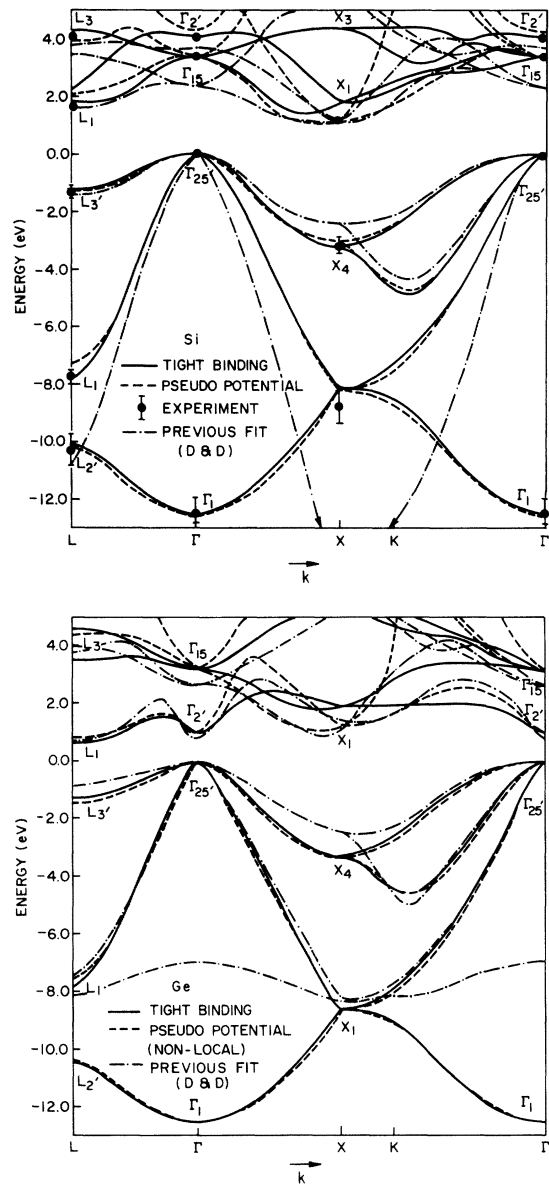


FIG. 4. (a) Present tight-binding fit to the energy bands of Si using seven first- and second-neighbor parameters is compared with pseudopotential energy bands (cf. Ref. 1) and an earlier 13-parameter first- and second-neighbor fit. (Dresselhaus and Dresselhaus, Ref. 32.) The latter, in spite of its abundance of adjustable parameters, is unsuitable for surface calculations for reasons described in the text. (b) Present tight-binding fit to the energy bands of Ge is compared to a recent nonlocal pseudopotential calculation [K. C. Pandey and J. C. Phillips, Phys. Rev. B 9, 1552 (1974)], and an earlier thirteen-parameter tight-binding fit (Ref. 32).

The determination of tight-binding parameters by a least-squares relaxation procedure is not unique. We searched for two months before set-

ting on the parameters listed in Table I. First we surveyed several alternative parametrization schemes, including d states as well as nonorthogonality parameters (see below). When we finally settled on the seven parameters listed in Table I, we did so because we felt our search had indicated that we had reached a point of abruptly diminishing returns, i. e., these parameters gave a distinctly better fit than could be obtained with fewer parameters, whereas additional parameters did not reduce the rms error appreciably. However, even with seven parameters one can easily find different local minima in the parameter space. We found many of these, with typical rms errors twice as large as those for the set shown in Table I. The key step which enabled us to find the parameters in Table I was the assumption that the starting parameters (in the least-squares relaxation process) satisfied the relation

$$(ss)_1(pp\sigma)_1 = (sp\sigma)_1^2, \quad (\text{A1})$$

which is approximately satisfied by the final parameters shown in Table I. While we have not been able to prove that the deep minimum is unique, our search never uncovered a parameter set with comparable accuracy. We regard Eq. (A1) as a useful supplement to the usual two-center approximation.²¹

A general aspect of our results was the fact that we could never obtain an accurate fit to the conduction bands. (In practice, to obtain good results for the dangling bond states we found it necessary to include the lowest conduction band energy levels in our set of fitted levels, but they were assigned only half the weight of the valence band states. This was consistent with the fact that our rms error for the lowest conduction band levels was about 0.5 eV, i. e., about twice as large as for the valence band states.)

We believe that there are several intrinsic reasons for this. First, there is the traditional argument based on the uncertainty principle and Wannier states. One argues that the omitted higher states in the conduction band mix with the lower conduction-band states to such an extent that localized basis functions, i. e., pseudoatomic orbitals are difficult to form for the conduction band. For the valence band, however, it is easier to form Wannier states because they are separated from the omitted states by an energy gap.

This argument is qualitatively correct, but it does not describe the central result common to all our fitted band structures. These gave a reasonably good fit to the lowest conduction band, but the total conduction bandwidth is always too small. One can understand why this is the case by constructing bond (+) and antibonding (-) s and p states, and ordering the energies $E(s+)$, $E(p+)$, $E(p-)$, and $E(s-)$. De-

fine the pseudo-Fermi energies by $2E_F^s = E(s+) + E(s-)$ and $2E_F^p = E(p+) + E(p-)$. Suppose $E_F^s \approx E_F^p$; in this case the conduction bandwidth $E(s-) - E(p-)$ is approximately equal to the valence bandwidth $E(p+) - E(s+)$. In the isolated atoms E_F^s and E_F^p are the (transition state) s and p energies, E^s and E^p . In the real crystal, however, the actual s - and p -like states contain large admixtures of higher plane-wave-like states, and because the conduction and valence bands contain equal numbers of electrons, the conduction band (where the free-electron density of states is higher) must be somewhat narrower. In practice the true conduction bands are not actually so narrow as is implied by $E_F^s = E^s$ and $E_F^p = E^p$. To compensate for this discrepancy within the TB framework, one must take $E_F^p - E_F^s < E^p - E^s$ and at the same time let the conduction band be still too narrow; in this way one obtains the best over-all fit to the valence bands and the lowest conduction band.

By recognizing these difficulties we have been able to find an accurate fit to the valence bands and a reasonably accurate fit to the lowest conduction band. Our entire procedure seems to differ essentially from what is commonly done in molecular calculations, because we have not used Slater functions to calculate matrix elements, and obtained energy levels from these. (Instead we go directly to the energy levels, and work inductively to find the matrix elements.) We have given serious consideration to the molecular approach, in part because we intend to extend these calculations to cases of chemisorption. In what follows we make a brief comparison of our methods with the more traditional molecular ones.

Some successful Hückel theories²³ have been based on very careful fits to the valence levels of CH_4 and C_2H_6 obtained either spectroscopically or from *ab initio* molecular orbital calculations.²⁷ In the case of ethane (C_2H_6) to obtain a good fit to the s and p valence levels it is necessary, if the wave functions are also reasonable, to use an extended Hückel method,²³ i. e., to include the effects of nonorthogonality of atomic orbitals. The difficulties are especially great for the splitting of the two lowest valence levels, which have s bonding and antibonding symmetry. In the CNDO method (which neglects nonorthogonality) this splitting²⁸ is about 12 eV; in *ab initio*²³ extended Hückel calculations^{23,29} it is about 5 eV, and experimentally³⁰ it is about 3.5 eV.

We have re-examined this problem by treating the matrix elements of the Hamiltonian and the overlap matrix S as adjustable (rather than derived from Slater functions) and have otherwise made approximations of the two-center, extended Hückel type. The results are similar to those obtained by previous workers, i. e., it is necessary to in-

clude nonorthogonality to obtain good results for tetrahedrally bonded ethane. On the other hand, a similar approach to the energy bands of tetrahedrally bonded Si led us to conclude that the non-orthogonality terms ($S_{ij} \neq 0$ for $i \neq j$) did *not* materially improve our results, i. e., the approximation $S_{ij} = \delta_{ij}$ is appropriate for the valence bands of Si. The following discussion attempts to explain qualitatively why the nonorthogonality terms are necessary in the molecular context but are not useful as adjustable parameters in fitting to the bulk crystalline energy bands.

The central difference between overlapping C atomic orbitals in C_2H_6 and the same overlapping effects for C orbitals in diamond is that in the latter structure each C atom has four nearest neighbor C atoms (rather than one, as in ethane). Thus in the crystal certain elements of S_{ij} ($i \neq j$) become larger than unity when calculated using conventional Slater orbitals, whereas with the same approximations S_{ij} is well-behaved in molecules. (This problem has been previously discussed by Slater³¹ and Inglis³¹ who described it as a "non-orthogonality catastrophe.")

The difficulties associated with large overlap terms can be circumvented formally by using as basis functions orthogonalized atomic orbitals. This mathematical procedure does not, however, explain why a good fit to the energy levels of disilane (Si_2H_6) requires $S_{ij} \neq 0$ ($i \neq j$), whereas a good fit to the valence bands of Si can be achieved with S diagonal. What is needed is a qualitative physical argument. One such argument is the following: In the molecule a large part of the solid angle around each atom "looks" like vacuum, and hence the optimized local orbital, i. e., that which gives the lowest energy for the system, will be only slightly contracted relative to the free atom, because, e. g. of the C-C covalent bond in ethane. At the same time, $S_{ij} \leq \frac{1}{2}$ ($i \neq j$) so that the off-diagonal elements of S are useful fitting parameters. In the crystal, these off-diagonal elements become so large that inversion of S is not well defined, and the optimized local orbitals are not obtainable simply from atomic orbitals, for instance by a scaling contraction. Nevertheless, the equilibrium lattice constant in diamond or Si is determined primarily by nearest-neighbor interactions, so that the lowest energy in a covalently bonded system is achieved by maximizing the effect of the nearest-neighbor Hamiltonian overlap terms H_{ij} ($i \neq j$, i and j centered on nearest neighbors) on the valence bands. Interaction with the more distant neighbors has only a secondary effect on the valence bands and on the covalent energy gap between valence and conduction bands (e. g., it determines the energy differences between zincblende, chalcopyrite, and wurtzite struc-

tures). Thus it is reasonable to fit the valence bands with general first neighbor terms. Because the atomic p energy is higher than the s energy, the only correction terms needed are p - p interactions between second neighbors.

The significance of the preceding qualitative remarks can best be brought out by comparison with the approaches of other workers, which have been based on considerations of mathematical completeness rather than physical relevance. For example, one occasionally sees it claimed that Wannier functions (or some generalization of them) can be profitably utilized as basis functions. In monatomic cases a Wannier function is essentially nothing more than an orthogonalized atomic orbital. In diatomic cases the Wannier function is localized in some unit cell, and if in the diamond lattice the unit cell is centered midway between two atoms, then it is easy to see that a Wannier valence-band function will be quite peculiar in the bonding regions connecting one atom in the unit cell to a nearest neighbor outside the unit cell. This appears to be a general defect of the Wannier prescription for constructing basis functions for covalent systems, or indeed for any crystal with more than one atom per unit cell.

It is of interest to compare the results of our fitting procedure, based on seven parameters, overdetermined in a statistical manner, with 13-parameter fit³² based on algebraic relations between the parameters and valence- and conduction-band experimental data. In the thirteen-parameter fit all first- and second-neighbor parameters H_{ij} allowed by crystal symmetry are included, without regard to the two-center approximation.²¹ For the first-neighbor interactions, the two-center approximation leads to no simplifications, but for second neighbors several terms vanish. It is interesting that in the 13-parameter fits³² to Si and Ge several of the largest second-neighbor terms are those which vanish in the two-center approximation. This unphysical behavior arises from the use of conduction-band experimental data; as we have seen, the SETBM does not give a good fit to the conduction bands. However, it might be argued that more parameters always give a better fit. That this is far from being the case is shown in Figs. 4(a) and 4(b), which compare our overdetermined seven-parameter fits with the 13-parameter fits for Si and Ge. The latter are very poor, especially towards the bottom of the valence band. Again, it might be argued that because the data which we fitted concerned primarily the highest valence band and the first two conduction bands, a fair test of the 14-parameter fit would involve primarily only those bands.³³ The dangling bond states apparently fit this prescription. We therefore compare in Table III the energies of the

dangling bond levels for \vec{k}_s at several symmetry points for the unrelaxed (111) surface calculated with our seven-parameter fit with those obtained with the 13-parameter fit.³⁴ Because our results in the relaxed case agree with self-consistent calculations³ (whose approach reproduces the bulk

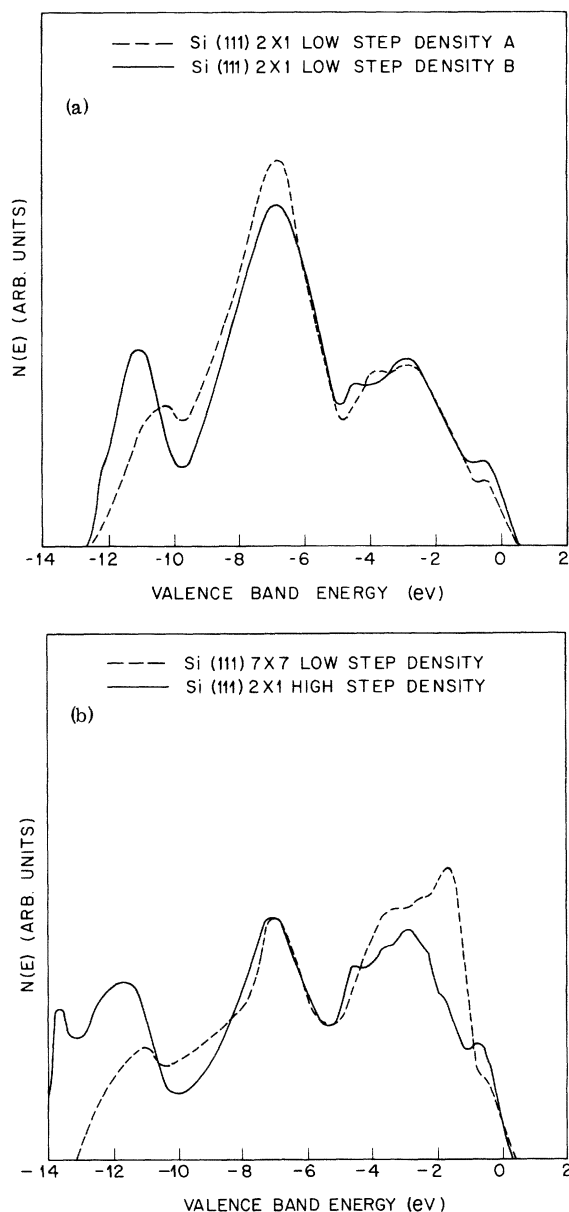


FIG. 5. (a) Comparison of dN/dE obtained from a photoemission study (Refs. 10 and 36) with $\hbar\omega = 21.2$ eV and a cylindrical acceptance geometry on cleaved Si(111) samples with low-step densities, but different ratios of primaries to secondaries, after subtraction of the latter. (b) Similar to (a), except that a low-step-density sample has been annealed (7×7 reconstruction pattern), and is contrasted with a high-step-density sample.

TABLE III. Dangling-bond energies in eV for unrelaxed (semi-infinite) Si based on the present seven-parameter fit to the bulk bands and a thirteen-parameter fit (see Refs. 32 and 34). Both cases include first and second neighbor interactions, but the bulk parameters differ because of the differences in the fitting procedure discussed in the text.

\vec{k}_s	SETBM(7)	SETBM(13)
Γ	0.30	0.60
J	-0.28	-0.40
K	-0.28	-0.64

band structure by the pseudopotential method, which is wholly different from the SETBM) to within 0.1 eV, we naturally ascribe the differences in a dangling bond energies for the unrelaxed case to the over-all poorness of the 13-parameter fit to the bulk energy bands. Indeed, because the perturbation at the surface is of order 10 eV, i. e., about half the total s - p band width, a good fit to the highest bulk valence and lowest conduction bands is not sufficient to produce good dangling bond bands, even though these bands lie between the afore-said bulk bands. Note in particular that the 13-parameter fit gives a dangling bond surface band width which is too large by about a factor of two. This discrepancy can be traced to an unphysical choice of parameters, which gives rise to spurious interactions which are manifested when one component of \vec{k} becomes imaginary, i. e., $\vec{k} = \vec{k}_s + i\kappa_n$. In particular, the thirteen-parameter value of the most basic parameter $E_p - E_s$ in Si is 11.8 eV, about two and a half times our value of 4.4 eV. By contrast, the value of $E_p - E_s$ used in semiempirical molecular orbital calculations³⁵ is 6.8 eV. *Ceteris paribus*, one would expect the apparent s - p splitting in the crystal to be somewhat smaller (the stronger interatomic interactions in the crystal quench the orbital angular momentum somewhat more effectively than in the molecule), in agreement with our choice of $E_p - E_s$. (For Ge the $3d$ case states hybridize slightly in the crystal with the $4p$ valence states, giving rise to a repulsive p - d interaction and a somewhat larger s - p splitting. In recent molecular work,³⁵ the value of the s - p energy difference in Ge is quoted as 7.35 eV, which exhibits the same trend relative to Si as our values do.) (See Note added in Proof.)

APPENDIX B: VALENCE-BAND DENSITIES OF STATES FROM PHOTOEMISSION

There is a growing body of experimental evidence^{8,10} that indicates that the apparent density of states of the valence band obtained in an ultraviolet photoemission experiment can change substantially with surface conditions (good cleave with low step density, poor cleave with high step densi-

TABLE IV. Listing of peak energies in dN/dE . The labels identify the following (in order): the theoretical curve with $l=3 \text{ \AA}$ in Fig. 2; similarly with $l=13 \text{ \AA}$; the dashed curve in Fig. 5(a); the solid curve in Fig. 5(a); the dashed curve in Fig. 5(b); the solid curve in Fig. 5(b); and a photoemission curve at 25 eV (Ref. 37). The abbreviations LSD and HSD refer to samples cleaved with low- and high-step densities, respectively.

3 \AA	0.3	-2.6	-7.4	-10.6	
13 \AA	0.3	-2.4	-7.2	-10.0	
LSD A	-0.5	-2.9	-6.7	-10.4	
LSD B	-0.5	-2.9	-6.9	-11.1	
LSD 7	-0.5	-1.6	-7.0	-10.9	
HSD	-0.9	-2.9	-7.1	-11.6	-13.6
25	-0.9	-3.4	-7.3	-11.3	

ty, and of course different cleavage faces, cleaved or annealed surfaces, as well as surface contamination). Because Si oxidizes so readily, a satisfactory survey of the remaining factors has not yet been made, but in this appendix a beginning of the discussion is made. The significance of the theoretical calculations of the surface density of states can be assessed more accurately when the various experimental factors are also illustrated.

The first problem that one must deal with in obtaining an ODS is to subtract the secondary background. In Fig. 5(a) we compare experimental results³⁶ on different samples which gave different amounts of secondary compared to primary emission. There are differences in the apparent density of states below -10 eV because in this region the secondary background is very larger. However, above -10 eV the two curves are in generally good agreement and the differences between them represent the kinds of variations between Si(111) samples that are obtained with different cleaves. Overall these differences are small.

In Fig. 5(b) we show how the results change from Fig. 5(a) when the cleaved, low-step-density Si(111) 2×1 surface is annealed to produce the 7×7 structure. The main change is that the height of the peak near -7.5 eV is now comparable to that of the peaks near -3 eV , whereas the 2×1 low-step-density structure of Fig. 5(a) gave a ratio of nearly 2 to 1. The same adjustment of peak heights can also be achieved with a cleaved surface using a poor cleave with a high step density, as illustrated in the figure. Note

that with a high-step density there is strong evidence that very deep back-bonding states are formed³⁶ near the steps for energies near -13.4 eV . Near steps the density of dangling bonds increases, and one would expect stronger back-bonding effects.

The theoretical ODS shown in Fig. 2 exhibits a ratio of peak heights near -7.5 eV compared to -3 eV of less than one. The emphasis on the -7.5 eV peak appears to decline with increasing photon energies³⁷ up to $\hbar\omega = 25 \text{ eV}$, at which energy a poorly cleaved (111) surface with a high-step density gives³⁷ a peak height ratio of about 0.8. This is consistent with the results³⁶ of Figs. 5(a) and 5(b), taken at a photon energy of 21.2 eV .

One can observe that the back-bonding effects near steps seem to change the shape of the spectrum primarily by adding a new peak near -13.5 eV . It is possible, therefore, that the primary cause of the variation in peak heights (-7.5 eV compared to -3 eV) between low-step-density and high-step-density cleaved surfaces shown in Figs. 5(a) and 5(b) arises from angular anisotropy of the escape probability.³⁶ With surface vacancies anisotropy would come into play in much the same way as one could obtain with high-step density, and thus the Lander model for the 7×7 surface is made more plausible.⁹

Although peak heights are found to vary substantially with surface conditions, on clean surfaces the peak locations are always very similar.³⁶ We have therefore collected in Table IV certain peak energies in the valence band dN/dE , and compared these with those of the theoretical curves in Fig. 2.

Note added in proof: After this paper was submitted for publication, some tight-binding calculations were reported [D. J. Chadi and M. L. Cohen, Phys. Status Solidi B 68, 405 (1975)] with substantially different values of $E_p - E_s$ (7.2 and 8.4 eV , in Si and Ge, respectively). However, in Figs. 6 and 8 of this paper the comparison between tight-binding and pseudopotential energy bands for high-symmetry directions seems to be as favorable as we show in our Fig. 4. This is because of their addition of a second-neighbor interaction which does not satisfy the two-center approximation, but which does improve the fit along (only) these special directions. Without this artificial term errors of an order of 1 eV are found with the first-neighbor parameters only.

¹K. C. Pandey and J. C. Phillips, Solid State Commun. 14, 439 (1974).

²K. C. Pandey and J. C. Phillips, Phys. Rev. Lett. 32, 1433 (1974).

³J. A. Appelbaum and D. R. Hamann, Phys. Rev. Lett. 31, 106 (1973); 32, 225 (1974).

⁴J. A. Pople and D. L. Beveridge, Approximate Molecular Orbital Theory (McGraw-Hill, New York, 1970).

⁵J. A. Appelbaum, in Surface Physics of Crystalline Materials, edited by J. M. Blakely (Academic, New York, to be published). Appelbaum concludes that most of the difference between inner and outer potentials

- arises from exchange and correlation energies.
- ⁶J. E. Rowe and H. Ibach, *Phys. Rev. Lett.* **31**, 102 (1973).
- ⁷J. C. Phillips and J. A. Van Vechten, *Phys. Rev. Lett.* **30**, 220 (1973).
- ⁸W. D. Grobman and D. E. Eastman, *Phys. Rev. Lett.* **29**, 1508 (1972). The ODS is obtained by averaging several photoemission energy distributions $N(E_i, \hbar\omega)$ over different photon energies to obtain $N(E_i)$, where E_i is the initial energy of the excited electrons.
- ⁹J. C. Phillips, *Surf. Sci.* **40**, 459 (1973).
- ¹⁰J. E. Rowe and H. Ibach, *Phys. Rev. Lett.* **32**, 421 (1974).
- ¹¹D. E. Eastman, *Sol. State Commun.* **8**, 41 (1970).
- ¹²J. Tejada *et al.*, *Phys. Status Solidi B* **58**, 189 (1973).
- ¹³N. V. Smith and M. M. Traum (unpublished).
- ¹⁴H. D. Hagstrum and G. E. Becker, *Phys. Rev. B* **8**, 1580, 1592 (1973).
- ¹⁵For reasons which are not entirely understood, the procedure for unfolding Auger electron distributions which is described in Ref. 14 requires a cutoff in the unfolded density of states 0.15 eV below the valence-band maximum. For Si(111) 7×7 , the INS and UPS results correspond very well in the region $-4 \text{ eV} < E < 0$ if this shift is eliminated in the INS curve for $N(E)$.
- ¹⁶In the curve shown for $N(E)$ by UPS in Fig. 4, secondaries have been subtracted in the usual way, as described for instance in Ref. 10.
- ¹⁷V. Bortolani, C. Calandra, and M. J. Kelly, *J. Phys. C* **6**, L349 (1973).
- ¹⁸J. C. Phillips, *Phys. Rev.* **104**, 1263 (1956).
- ¹⁹We are grateful to L. Kleinman for stressing in private conversations that "flat bands" are equivalent to having 1.00 electron per dangling bond [also L. Kleinman (unpublished)].
- ²⁰E. Caruthers, L. Kleinman, and G. P. Alldredge, *Phys. Rev. B* (to be published).
- ²¹J. C. Slater and G. F. Koster, *Phys. Rev.* **94**, 1498 (1954).
- ²²E. Hückel, *Z. Phys.* **60**, 423 (1930).
- ²³R. Hoffman, *J. Chem. Phys.* **39**, 1397 (1963).
- ²⁴P. E. Stevenson and W. N. Lipscomb, *J. Chem. Phys.* **52**, 5343 (1970).
- ²⁵E. B. Moore, Jr. and C. M. Carlson, *Phys. Rev. B* **6**, 2063 (1971).
- ²⁶R. P. Messmer, *Chem. Phys. Lett.* **11**, 589 (1971).
- ²⁷L. C. Snyder and H. Basch, *Molecular Wave Functions and Properties* (Wiley, New York, 1972).
- ²⁸H. Fischer and H. Kollman, *Theor. Chim. Acta* **13**, 210 (1969).
- ²⁹W. E. Palke and W. N. Lipscomb, *J. Am. Chem. Soc.* **88**, 2384 (1966).
- ³⁰K. Hamrin *et al.*, *Chem. Phys. Lett.* **1**, 613 (1968).
- ³¹J. C. Slater, *Phys. Rev.* **35**, 509 (1930); D. R. Inglis, *ibid.* **46**; 135 (1934).
- ³²G. Dresselhaus and M. S. Dresselhaus, *Phys. Rev.* **160**, 649 (1967).
- ³³Even with 14 adjustable parameters, the first direct edge in Si was found at 2.4 eV, whereas experimentally it lies at about 3.4 eV. The bandwidth of the conduction band is unavoidably too narrow in the SETBM, so that fitting to the indirect gap in Si (1.1 eV) makes the direct gap always too small.
- ³⁴K. Hirabayashi, *J. Phys. Soc. Jpn.* **27**, 1475 (1969).
- ³⁵D. P. Santry and G. A. Segal, *J. Chem. Phys.* **47**, 158 (1967); H. L. Hase and A. Schwieg, *Theor. Chim. Acta* **31**, 215 (1973).
- ³⁶J. E. Rowe (private communication and/or unpublished data).
- ³⁷D. E. Eastman (private communication and/or unpublished data).